

# Surface shape and local critical behaviour in two-dimensional directed percolation

C Kaiser and L Turban

Laboratoire de Physique du Solide†, Université Henri Poincaré (Nancy I), BP 239,  
F-54506 Vandœuvre lès Nancy Cedex, France

Received 23 September 1994

**Abstract.** Two-dimensional directed site percolation is studied in systems directed along the  $x$ -axis and limited by a free surface at  $y=\pm Cx^k$ . Scaling considerations show that the surface is a relevant perturbation to the local critical behaviour when  $k < 1/z$  where  $z=\nu_{\parallel}/\nu$  is the dynamical exponent. The tip-to-bulk order parameter correlation function is calculated in the mean-field approximation. The tip percolation probability and the fractal dimensions of critical clusters are obtained through Monte-Carlo simulations. The tip order parameter has a nonuniversal,  $C$ -dependent, scaling dimension in the marginal case,  $k=1/z$ , and displays a stretched exponential behaviour when the perturbation is relevant. The  $k$ -dependence of the fractal dimensions in the relevant case is in agreement with the results of a blob picture approach.

## 1. Introduction

The shape of the free surface limiting a system may influence its local critical behaviour at a bulk second order phase transition, provided the deviation from the flat surface is long range. For corners in two dimensions, wedges or cones in three dimensions, a marginal behaviour is obtained, with local critical exponents depending on the opening angle, in isotropic critical systems [1–9]. This result is linked to the invariance of the shapes under isotropic rescaling (see [10] for a review).

With parabolic shapes, the surface introduces a relevant perturbation to the flat surface fixed point leading, locally, to stretched exponential behaviour for the order parameter and the correlation functions [11]. The Ising model [11–13], the self-avoiding-walk [14] and ordinary percolation [15] have been studied for this geometry in two dimensions.

In anisotropic systems the correlation length diverges as  $\xi_{\parallel} \sim t^{-\nu_{\parallel}}$  along a time-like direction and as  $\xi_{\perp} \sim t^{-\nu}$  in the transverse directions with a dynamical exponent  $z=\nu_{\parallel}/\nu$  [16]. Covariance under a change of the length scales then requires two different scaling factors,  $b_{\parallel}=b^z$  and  $b_{\perp}=b$  [17]. In this way, the relation between the correlation lengths  $\xi_{\parallel} \sim (\xi_{\perp})^z$  is preserved. As a consequence, scale invariant shapes are different from the isotropic case: they now correspond to parabolic-like surfaces [18]. For example, the marginal shape for the directed walk, with  $z=2$ , is the true parabola in two dimensions, a paraboloid or a parabolic wedge in three dimensions [18,19].

† Unité de Recherche Associée au CNRS No 155

In the present work, we study the two-dimensional directed site percolation problem inside a parabolic-like system. The scaling behaviour is discussed in section 2. The problem is solved in a mean-field approximation in section 3. The results of Monte-Carlo simulations are presented in section 4 and we end with a discussion in section 5.

## 2. Scaling considerations

We consider a system displaying anisotropic critical behaviour and limited by a free surface at  $y = \pm Cx^k$  in the  $(x, y)$ -plane where  $x$  is the time-like coordinate. Under rescaling, with  $x' = x/b^z$  and  $y' = y/b$ , the geometrical constant  $C$  transforms according to

$$\frac{1}{C'} = b^{1-zk} \frac{1}{C}. \quad (2.1)$$

When  $k > 1/z$ ,  $1/C$  renormalizes to zero, i. e. the system flows towards the flat surface geometry. The perturbation introduced by the free surface is irrelevant with respect to the flat surface fixed point. On the contrary, when  $k < 1/z$ ,  $1/C$  grows under rescaling and the system becomes locally narrower. The perturbation is then relevant and one expects a strong reduction of the order at the tip associated with a new type of local critical behaviour. The value  $k = 1/z$  corresponds to a scale-invariant shape leading to a marginal local critical behaviour with  $C$ -dependent exponents. For an isotropic system,  $z = 1$  and the marginal shape, with  $k = 1$ , corresponds to the corner geometry mentioned above.

Let  $m_0$  be the tip order parameter, with scaling dimension  $x_m$  at the flat surface fixed point, on a finite system with size  $L$  along the  $x$ -axis. Under a change of scale, it transforms as

$$m_0 \left( t, \frac{1}{C}, \frac{1}{L} \right) = b^{-x_m} m_0 \left( b^{1/\nu} t, \frac{b^{1-zk}}{C}, \frac{b^z}{L} \right) \quad (2.2)$$

where  $t$  is the thermal scaling field and  $1/C$ , which is vanishing at the reference fixed point like  $1/L$  in finite-size scaling, is treated as a new scaling field introduced by the parabolic free surface. One may also notice that, for a directed problem, the system does not see a flat free surface at  $x = 0$  and  $x_m$  is also the bulk scaling dimension of the order parameter.

Taking  $b = t^{-\nu}$ , one obtains

$$m_0 \left( t, \frac{1}{C}, \frac{1}{L} \right) = t^\beta m_t \left( \frac{l_C}{t^{-\nu_\parallel}}, \frac{L}{t^{-\nu_\parallel}} \right), \quad l_C = C^{z/(1-zk)} \quad (2.3)$$

where  $\beta = \nu x_m$  and the shape of the system introduces a new length scale given by  $l_C$  as long as the shape is not scale-invariant, i. e.  $k \neq 1/z$ . In the same way, taking  $b = l_C^{1/z}$  in equation (2.2), one obtains the following finite-size scaling behaviour at the critical point  $t = 0$ :

$$m_0 \left( 0, \frac{1}{C}, \frac{1}{L} \right) = l_C^{-x_m/z} m_C \left( \frac{L}{l_C} \right). \quad (2.4)$$

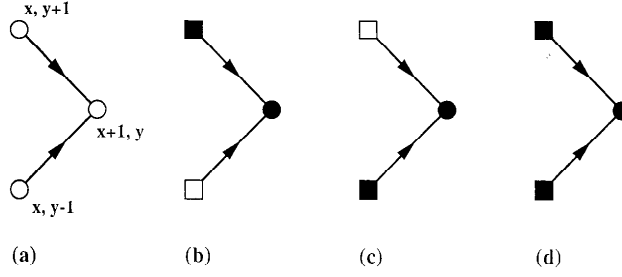


**Figure 1.** Directed site percolation on the square lattice: (a) The system is directed along the diagonal of the square lattice. (b–d) The site at  $(x+1, y)$  (full circle) is connected to the origin if at least one of its nearest neighbours at  $x$  is connected to the origin (full squares).

In the marginal case,  $z = 1/k$ , the scaling dimension of the tip order parameter becomes  $C$ -dependent and equation (2.2) is changed into

$$m_0 \left( t, \frac{1}{C}, \frac{1}{L} \right) = b^{-x_m(C)} m_{\text{marg}} \left( b^{1/\nu} t, \frac{b^z}{L} \right). \quad (2.5)$$

The order parameter correlation function between the origin and a point at  $(x, y)$  transforms as

$$G \left( t, x, y, \frac{1}{C} \right) = b^{-2x_m} G \left( b^{1/\nu} t, \frac{x}{b^z}, \frac{y}{b}, \frac{b^{1-zk}}{C} \right) \quad (2.6)$$

when  $L$  is infinite. With  $b = x^{1/z}$ , equation (2.6) leads to:

$$G \left( t, x, y, \frac{1}{C} \right) = x^{-2x_m/z} g \left( \frac{x}{t^{-\nu_{\parallel}}}, \frac{y^z}{x}, \frac{x}{l_C} \right). \quad (2.7)$$

These scaling forms will be used later to analyze the mean-field results and the Monte-Carlo data.

### 3. Mean-field approximation

We consider the site percolation problem on a square lattice, directed along a diagonal of the squares as shown in figure 1a, with a site occupation probability  $p$ . The order parameter correlation function is the probability density  $P(x, y)$  for a site at  $(x, y)$  to be connected to the origin. The site at  $(x+1, y)$  will be connected too if it is occupied and if at least one of its two nearest neighbours at  $x$  are themselves connected to the origin (figures 1b–d). In a mean-field approximation [20] where correlations between the  $P$ s on different sites are neglected, this occurs with probability

$$P(x+1, y) = p \left\{ P(x, y+1) [1 - P(x, y-1)] + P(x, y-1) [1 - P(x, y+1)] + P(x, y+1) P(x, y-1) \right\} \quad (3.1)$$

where the different terms on the right correspond to the last three diagrams in figure 1.

Going to the continuum limit and neglecting nonlinear terms involving derivatives, one is led to the following differential equation:

$$\frac{\partial P}{\partial x} = p \frac{\partial^2 P}{\partial y^2} + (2p - 1)P - pP^2. \quad (3.2)$$

The order parameter is the probability  $P_0$  for the site at the origin to belong to an infinite cluster. For the un-confined system, it is given by the homogeneous stationary solution of equation (3.2) as

$$P_0 = \begin{cases} \frac{2p-1}{p} & p \geq p_c = \frac{1}{2} \\ 0 & p < p_c \end{cases} \quad (3.3)$$

and vanishes at the percolation threshold  $p_c$  with an exponent  $\beta^{mf} = 1$ .

Below the threshold and far from the origin,  $P(x, y) \ll 1$  and equation (3.2) can be linearized, leading to:

$$\frac{\partial P}{\partial x} \simeq \frac{1}{2} \frac{\partial^2 P}{\partial y^2} + 2(p - p_c)P. \quad (3.4)$$

Through the change of function  $P(x, y) \rightarrow \exp[2(p_c - p)x]P(x, y)$  an ordinary diffusion equation is obtained, so that

$$P(x, y) = e^{-2(p_c - p)x} \frac{\exp\left(-\frac{y^2}{2x}\right)}{\sqrt{2\pi x}} \quad (3.5)$$

for the un-confined system. In  $d+1$  dimensions the power-law decay would be changed into  $x^{-d/2}$ . From a comparison with equation (2.7) where  $t$  is now  $|p - p_c|$ , one deduces the following exponents for directed percolation,

$$\nu_{\parallel}^{mf} = 1 \quad \nu^{mf} = 1/2 \quad z^{mf} = 2 \quad x_m^{mf} = \frac{d}{2} \quad (3.6)$$

where  $\nu^{mf}$  follows from scaling. The scaling law  $\beta = \nu x_m$  is verified for the mean-field (Gaussian) exponents only at the upper critical dimension  $d_c + 1$  which, according to (3.3) and (3.6), is equal to 5 for directed percolation.

On a parabolic system, we use the new variables  $x$  and  $\zeta(x, y) = y/x^k$  for which the free surface is shifted to  $\zeta = \pm C$  and equation (3.4) is changed into

$$\frac{\partial P}{\partial x} = \frac{1}{2x^{2k}} \frac{\partial^2 P}{\partial \zeta^2} + k \frac{\zeta}{x} \frac{\partial P}{\partial \zeta} + 2(p - p_c)P \quad (3.7)$$

with the boundary condition  $P(x, \zeta = \pm C) = 0$ . Through the change of function

$$P(x, \zeta) = \exp\left[-2(p_c - p)x - \frac{k}{2}\zeta^2 x^{2k-1}\right] Q(x, \zeta) \quad (3.8)$$

equation (3.7) leads to

$$\frac{\partial Q}{\partial x} = \frac{1}{2x^{2k}} \frac{\partial^2 Q}{\partial \zeta^2} + \frac{k}{2} \left[ (k-1)\zeta^2 x^{2k-2} - \frac{1}{x} \right] Q \quad (3.9)$$

for which the variables separate when  $k = 1, 1/2$  or  $0$ . According to equation (2.1), in mean-field, these values of  $k$  just correspond to irrelevant, marginal and relevant perturbations.

For  $k = 1$ , i. e. in the corner geometry, (3.9) gives

$$x^2 \frac{\partial Q}{\partial x} + \frac{x}{2} Q = \frac{1}{2} \frac{\partial^2 Q}{\partial \zeta^2} \quad \zeta = \frac{y}{x} \quad P = e^{-2(p_c - p)x - y^2/2x} Q \quad (3.10)$$

and the correlation function, which is even in  $y$ , takes the form

$$P(x, y) = e^{-2(p_c - p)x} \frac{\exp\left(\frac{-y^2}{2x}\right)}{\sqrt{2\pi x}} \sum_{n=0}^{\infty} A_n \exp\left[\frac{(2n+1)^2 \pi^2}{8C^2 x}\right] \cos\left[\frac{(2n+1)\pi y}{2Cx}\right]. \quad (3.11)$$

This is just the un-confined solution (3.5), modulated by a function which depends on the two last variables  $v$  and  $w$  of the scaling function  $g(u, v, w)$  in equation (2.7), with here  $z = 2$  and  $l_C = C^{-2}$ . The critical behaviour is the same as for un-confined percolation as expected for an irrelevant perturbation.

For the true parabola which is the marginal geometry, one may use equation (3.7) with  $k = 1/2$  to obtain

$$x \frac{\partial Q}{\partial x} = \frac{1}{2} \frac{\partial^2 Q}{\partial \zeta^2} + \frac{\zeta}{2} \frac{\partial Q}{\partial \zeta} \quad \zeta = \frac{y}{x^{1/2}} \quad P = e^{-2(p_c - p)x} Q \quad (3.12)$$

which is of the form studied in [18] for the directed walk problem. Writing  $Q(x, \zeta) = \phi(x)\psi(\zeta)$  leads to the following eigenvalue problem for  $\psi(\zeta)$

$$\frac{1}{2} \frac{d^2 \psi}{d\zeta^2} + \frac{\zeta}{2} \frac{d\psi}{d\zeta} = -\lambda^2 \psi \quad (3.13)$$

with  $\phi(x) \sim x^{-\lambda^2}$ . The solution, which is even and regular at the origin, can be written as a series expansion,  $\sum_{n=0}^{\infty} a_n \zeta^{2n}$ . According to (3.13), the coefficients satisfy

$$a_{n+1} = -\frac{(\lambda^2 + n)}{(n+1)(2n+1)} a_n \quad (3.14)$$

which is the recursion relation for the coefficients of the degenerate hypergeometric function

$${}_1F_1\left[\lambda^2, \frac{1}{2}; -\frac{\zeta^2}{2}\right] = 1 + \sum_{n=1}^{\infty} (-1)^n \frac{\lambda^2(\lambda^2+1)\cdots(\lambda^2+n-1)}{1.3\cdots(2n-1)} \frac{\zeta^{2n}}{n!}. \quad (3.15)$$

The boundary condition  $\psi(C) = 0$  gives the eigenvalues  $\lambda_n$  which are the zeros of  ${}_1F_1[\lambda_n^2, 1/2; -C^2/2]$ . The solution is obtained as the eigenvalue expansion

$$P(x, y) = e^{-2(p_c - p)x} \sum_{n=0}^{\infty} B_n x^{-\lambda_n^2} {}_1F_1\left[\lambda_n^2, \frac{1}{2}; -\frac{y^2}{2x}\right]. \quad (3.16)$$

The behaviour at large  $x$  is governed by the first term in this expansion which decays as  $x^{-\lambda_0^2}$ , i. e. with a  $C$ -dependent exponent as expected for a marginal perturbation.

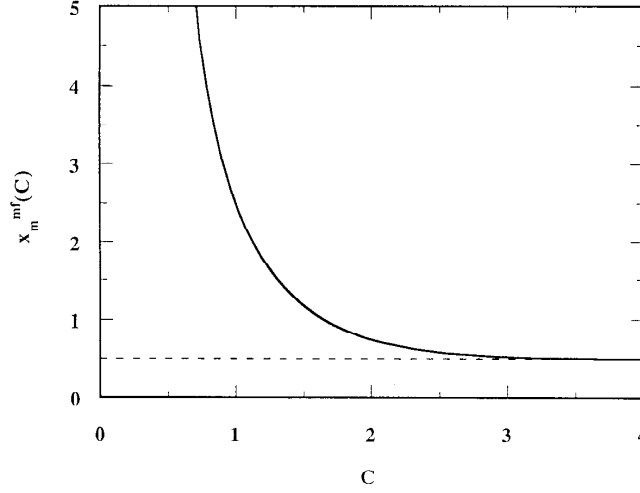


**Figure 2.** Scaling dimension of the tip order parameter as a function of  $C$  in the mean-field approximation when the shape is marginal. The local exponent  $x_m^{mf}(C)$  diverges when  $C \rightarrow 0$  and goes to its unperturbed value  $x_m^{mf} = 1/2$  when  $C \rightarrow \infty$ .

The dimension of the tip-to-bulk correlation function is the sum of the tip and bulk order parameter dimensions, the first one being variable. Comparing with the form of the decay in (2.7) gives  $\lambda_0^2 = [x_m^{mf}(C) + x_m^{mf}]/z^{mf}$  and, using (3.6), the tip order parameter dimension is given by

$$x_m^{mf}(C) = 2\lambda_0^2 - \frac{1}{2}. \quad (3.17)$$

Its dependence on  $C$  is shown in figure 2.

Analytical results can be obtained only in limiting cases which have already been discussed in [18]. When  $C$  is infinite,  $\lambda_0^2 = 1/2$ , only the first term in the expansion remains, which satisfies the initial and boundary conditions, giving back the free solution in equation (3.5) since  ${}_1F_1(\frac{1}{2}, \frac{1}{2}; -y^2/2x) = \exp(-y^2/2x)$ . For large  $C$ -values, the tip exponent takes the following form

$$x_m^{mf}(C) = \frac{1}{2} + \sqrt{\frac{2}{\pi}} C \exp\left(-\frac{C^2}{2}\right) [1 + O(\varepsilon)] \quad (3.18)$$

where  $\varepsilon$  is the correction term itself. For narrow systems, the hypergeometric function gives a cosine to leading order in  $C^2$ . One obtains the following asymptotic behaviour in  $x$

$$P(x, y) \sim x^{-\pi^2/8C^2} \cos\left(\frac{\pi y}{2C\sqrt{x}}\right) \quad (3.19)$$

and the tip exponent diverges as  $\pi^2/4C^2$ .

For the strip geometry, which corresponds to a relevant perturbation, one can use (3.9) with  $k=0$  or, more simply, go back to the original equation (3.4) giving

$$\frac{\partial Q}{\partial x} = \frac{1}{2} \frac{\partial^2 Q}{\partial y^2} \quad P = e^{-2(p_c - p)x} Q \quad (3.20)$$

The solution satisfying the initial condition  $P(0, y) = \delta(y)$  reads

$$P(x, y) = \frac{\exp[-2(p_c - p)x]}{C} \sum_{n=0}^{\infty} \exp\left[-\frac{(2n+1)^2 \pi^2 x}{8C^2}\right] \cos\left[\frac{(2n+1)\pi y}{2C}\right] \quad (3.21)$$

in agreement with the scaling form (2.7) for the mean-field exponents. The perturbation due to the free surface induces a simple exponential decay of the correlations at  $p_c$ . Actually, the system is now one-dimensional and this term corresponds to a shift of the percolation threshold by  $(\pi/4C)^2$ .

For  $0 < k < 1/2$ , the simple exponential is expected to be replaced by a stretched one, involving some power of the last scaling variable  $w = x/l_C$  in equation (2.7). The power goes to 1 when  $k=0$  and has to vanish when the system is marginal ( $k=1/2$ ) in order to give a  $C$ -dependent decay exponent. A good candidate for the asymptotic behaviour is [18]

$$P(x, y) = \frac{\exp[-2(p_c - p)x]}{Cx^k} \exp\left(-\frac{\pi^2}{8C^2} \frac{x^{1-2k}}{1-2k}\right) \cos\left(\frac{\pi y}{2Cx^k}\right). \quad (3.22)$$

It has the proper scaling form (2.7) with mean-field exponents and interpolates between the strip result (3.21) and the small- $C$  result (3.19) for the parabola.

#### 4. Monte-Carlo simulations

As in the mean-field approach of the last section, the Monte-Carlo (MC) simulations were performed for site percolation on a square lattice along the diagonal direction. Accurate estimates of the percolation threshold and directed percolation exponents have been deduced from series expansion in [21] with

$$\begin{aligned} p_c &= 0.705489(4) & \nu &= 1.097(2) & \nu_{\parallel} &= 1.734(2) \\ \gamma &= 2.278(2) & z &= 1.581(3) & \beta &= 0.276(3) \end{aligned} \quad (4.1)$$

where the last two values follow from scaling laws.

On the lattice, the sites inside or on the curve  $y = \pm Cx^k$  are considered to belong to the system. The tip order parameter was calculated on parabolic-like systems with size  $L$  along the  $x$ -axis. On these finite-size systems,  $P_0$  is the probability that a cluster grown from an occupied site at  $x=y=0$  reaches  $x=L$ . Such a cluster is called "infinite". "Finite" clusters are those dying before  $x=L$ .

In order to spare computer time the MC-algorithm ensures that a cluster reaches  $x=L$  as fast as possible. This is done by always trying to occupy those sites with the largest  $x$ -coordinate. The coordinates of sites from which the growth may eventually continue but which are closer to the origin are stored into a list of active sites. The growth stops once the size of the cluster is equal to  $L$ , even if it still contains active sites. Thus, the complete infinite cluster has not been built. Subsequently, if there are no active sites left, a complete finite cluster has been grown. An example is shown in figure 3.

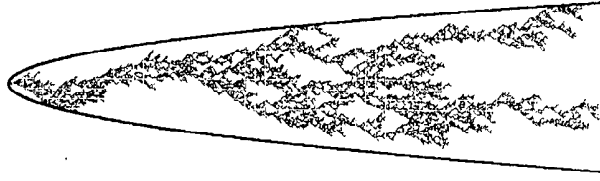


**Figure 3.** Directed percolation cluster generated using the Monte-Carlo algorithm described in the text. Here,  $L=1000$ ,  $k=1/2$  and  $C=4$ .

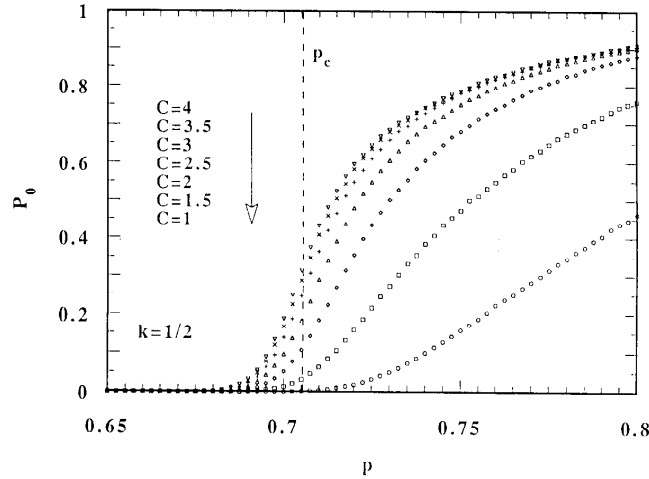


**Figure 4.** Tip percolation probability on a parabola ( $k=1/2$ ) with length  $L=1000$  as a function of  $p$ . The Monte-Carlo results are averaged over  $10^5$  samples for 7 values of  $C$  between 4 and 1 from top to bottom. The non-vanishing percolation probability at the percolation threshold (dashed line) indicates strong finite-size effects which are increasing with  $C$ .

With this algorithm, which is a modified version of the one used in [15] for ordinary percolation, the computation time for increasing  $p > p_c$  remains almost constant. Thus we could compute  $P_0$  as a function of  $p$  up to  $p=0.8$  ( $k=1/2, 1/z$ ) for  $L=1000$  taking averages over  $10^5$  samples. The results are shown in figures 4 and 5 for values of  $C$  ranging from 1 to 4.

Due to the anisotropy, finite-size effects remain important. This appears in the non-vanishing values of  $P_0(p_c)$  and increases with  $C$ , i. e. when the system opens. According to the scaling relation (2.3),  $P_0 t^{-\beta}$  is an universal function of  $l_C/\xi_{\parallel}$  and  $L/\xi_{\parallel}$ . This has been verified in the relevant case  $k=1/2$  for the first of these scaling variables. A good data collapse is obtained in figure 6 for  $C=1, 1.5, \dots, 4$  and  $L=50, 100, \dots, 1000$  with a fixed ratio  $L/\xi_{\parallel}=0.34$ .

In order to check the expected stretched exponential behaviour in the relevant case, we performed a finite-size scaling study at the critical point. The tip percolation probability, for  $k=1/2$  and  $1 \leq C \leq 4$ , was calculated at the percolation threshold on



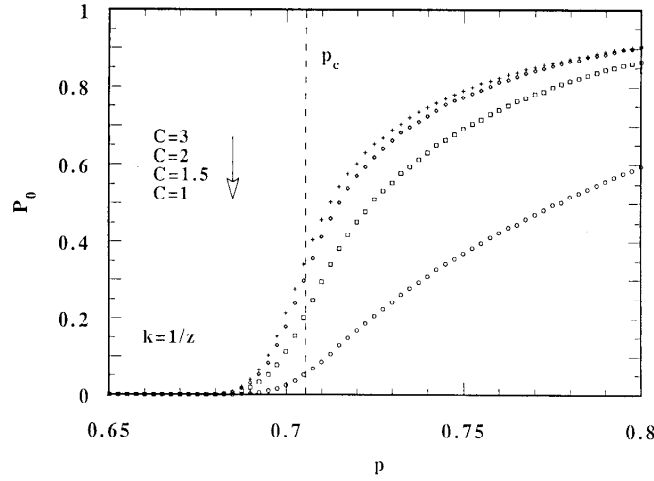


**Figure 5.** As in figure 4 for the marginal case,  $k=1/z$ .

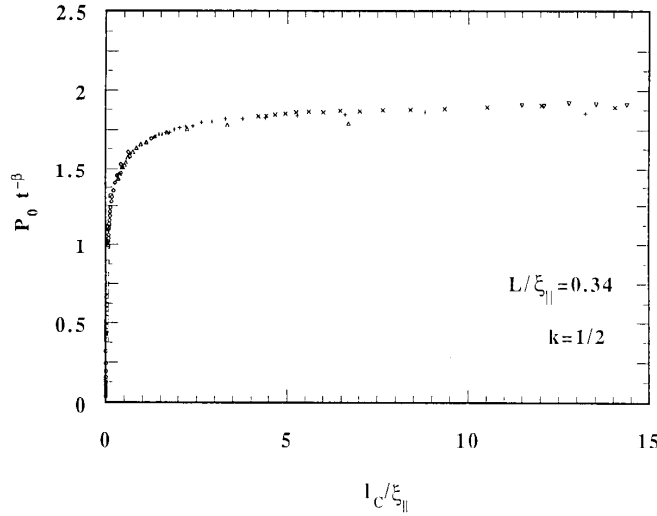


**Figure 6.** Scaling function  $P_0 t^{-\beta}$  versus  $l_C/\xi_{||}$  in the relevant case ( $k=1/2$ ). A good data collapse is obtained for the different values of  $C$  (same symbols as in figure 4).

systems with size  $50 \leq L \leq 1000$ , taking averages over  $10^5$  MC samples. According to equation (2.4),  $P_0 l_C^{x_m/z}$  is a function of  $L/l_C$  which depends only on  $k$ . The scaling behaviour is shown in figure 7 where the deviations at small  $C$ -values is likely to be due to corrections to scaling. Actually, the reference fixed point for which equation (2.4) was written corresponds to  $C \rightarrow \infty$ . In this semi-logarithmic plot, a linear dependence on  $(L/l_C)^{1-zk}$  is obtained. It corresponds to a stretched exponential behaviour for the scaling function  $m_C(L/l_C)$  although some power in front of the exponential cannot be excluded. Other simple combinations of  $z$  and  $k$  for the stretching exponent did not lead to a linear behaviour.

In the marginal case,  $k=1/z$ , the scaling dimension of the tip order parameter

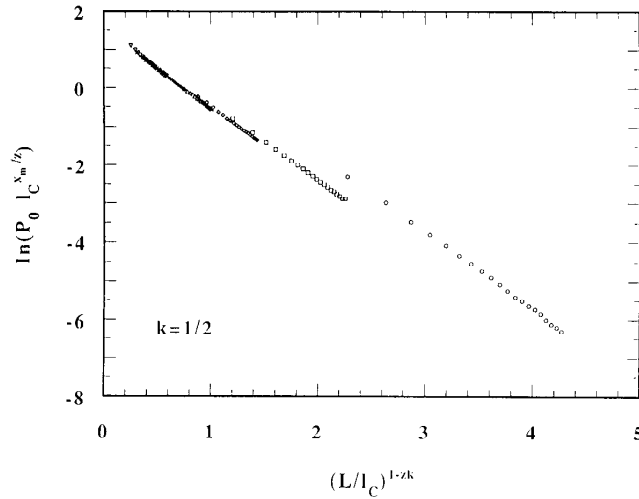


**Figure 7.** Finite-size scaling of the tip order parameter at the critical point for a relevant surface shape ( $k=1/2$ , same symbols as in figure 4 for  $C$ ). The almost linear variation of  $\ln P_0 l_C^{x_m/z}$  as a function of  $(L/l_C)^{1-zk}$  indicates a stretched exponential behaviour of the tip percolation probability.

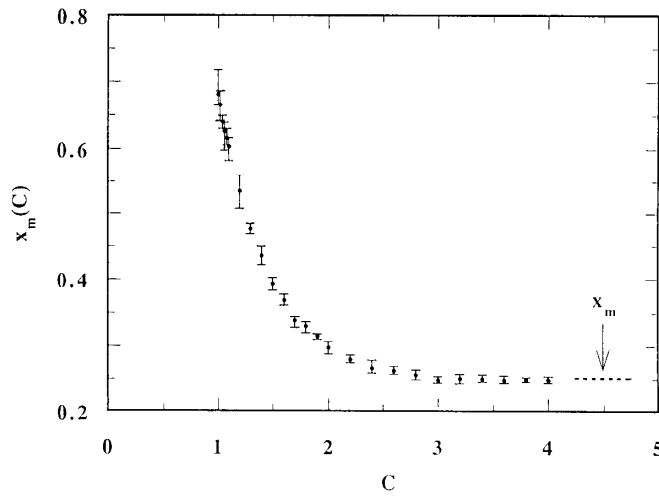


**Figure 8.** Scaling dimension of the tip order parameter as a function of  $C$  obtained through finite-size scaling when the shape is marginal ( $k=1/z$ ). The local exponent  $x_m(C)$  diverges when  $C \rightarrow 0$  and goes to its unperturbed value  $x_m = 0.252(3)$  when  $C \rightarrow \infty$ .

is expected to vary with  $C$ . Equation (2.5), with  $b = L^{1/z}$ , leads to the finite-size behaviour  $P_0(L) \sim L^{-x_m(C)/z}$  at  $p=p_c$  which can be used to determine  $x_m(C)$ . This has been done taking averages for  $P_0(L)$  over  $2.10^5$  samples with  $L=500, 520, \dots, 1000$ . The tip exponent was deduced from the asymptotic slopes of log-log plots. The results are shown in figure 8. The dependence on  $C$  is qualitatively similar to the mean-field one in figure 2: the scaling dimension diverges when  $C$  vanishes and it decreases to

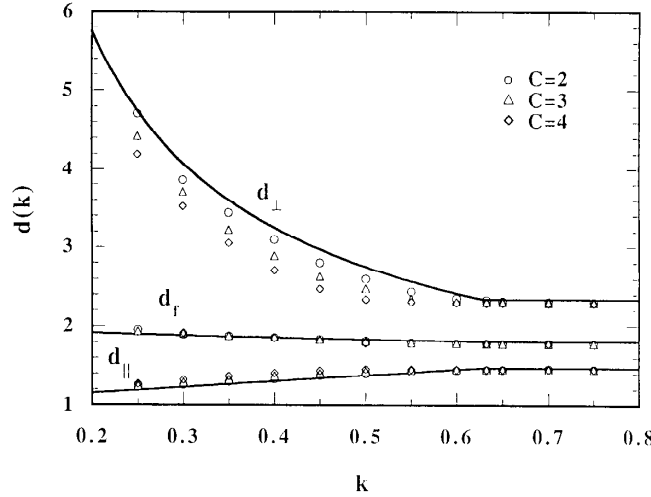


**Figure 9.** Fractal dimensions versus  $k$  for finite critical percolation clusters starting at the tip. The variation in the relevant regime,  $k < 1/z = 0.633(2)$ , is well described by the blob picture approach (lines) when  $C$  decreases. The deviations for large  $C$ -values are due to the finite size of the system: only a few blobs can develop and the fractal dimensions are then closer to the unperturbed ones.

the bulk value  $x_m = \beta/\nu = 0.252(3)$  when  $C$  goes to infinity.

The fractal structure of finite critical clusters was also studied. Since details can be found in reference [22], here we only give a brief summary of our results. As in figure 3,  $2.10^5$  percolation clusters starting from the tip were generated at the percolation threshold, inside a parabolic system with size  $L = 1000$  for  $C = 2, 3, 4$  and values of  $k$  ranging from 0.25 to 0.75. The mean square radii of gyration,  $\langle X_s^2 \rangle$  in the  $x$ -direction and  $\langle Y_s^2 \rangle$  in the transverse direction, were determined for  $s$ -site "finite" clusters, i. e. clusters with  $x_{max} < L$ .

For an unconfined system, the cluster size behaves as

$$s \sim \overline{X_s}^{d_{\parallel}} \sim \overline{Y_s}^{d_{\perp}} \quad (4.2)$$

where  $\overline{X_s} = \langle X_s^2 \rangle^{1/2}$ ,  $\overline{Y_s} = \langle Y_s^2 \rangle^{1/2}$ . The exponents are fractal dimensions which, extending an argument of Stauffer [23], are related to the directed percolation exponents through

$$d_{\parallel} = \frac{\beta + \gamma}{\nu_{\parallel}} = 1.473(2) \quad d_{\perp} = \frac{\beta + \gamma}{\nu_{\perp}} = 2.329(3). \quad (4.3)$$

The second value is greater than the dimension of the system due to the anisotropy as explained in reference [22]. A single fractal dimension  $d_f$  may be also defined using the characteristic length  $l \sim (l_{\parallel} l_{\perp})^{1/2} \sim s^{1/d_f}$  associated with the surface of the cluster so that [20]  $2/d_f = 1/d_{\parallel} + 1/d_{\perp}$  and then,  $d_f = 1.805(2) < 2$ .

Inside a parabolic system, one expects a similar behaviour with  $k$ -dependent fractal dimensions  $d_{\parallel}(k)$ ,  $d_{\perp}(k)$ , when the shape is a relevant perturbation. Log-log plots of the MC results are linear for cluster sizes between  $2^6$  and  $2^{12}$ - $2^{13}$ . Deviations

at larger sizes are due to finite-size effects. The fractal dimensions are shown in figure 9 as functions of  $k$ . The form of the variation in the relevant regime,  $k < 1/z$ , can be obtained using a blob picture approach [24–26,14]. The cluster configuration is supposed to follow from the piling up of anisotropic blobs inside the parabolic system. Within each blob the structure is the same as for unconfined clusters with the unperturbed values of the fractal dimensions. In this way one obtains [22]

$$d_{\parallel}(k) = 1 + zk(d_{\parallel} - 1), \quad d_{\perp}(k) = \frac{d_{\parallel}(k)}{k}, \quad 0 < k \leq 1/z \quad (4.4)$$

in good agreement with the Monte-Carlo data as shown in figure 9.

## 5. Conclusion

The local critical behaviour for directed percolation has been investigated at the tip of two-dimensional parabolic-like systems. The problem has been treated using mean-field theory and MC-simulations. In the marginal case,  $k = 1/z$ , the percolation probability and the order parameter correlation function display a non-universal local critical behaviour: the local exponents vary continuously with the shape of the system. In the relevant case,  $k < 1/z$ , the critical tip percolation probability is a stretched exponential function of the reduced size  $L/l_C$  and finite critical clusters have  $k$ -dependent fractal dimensions.

Although we were unable, due to strong finite-size effects, to check a similar stretched exponential dependence on  $\xi_{\parallel}/l_C$  in the relevant case, the following general picture seems to emerge from our mean-field and MC results, exact and MC results for the Ising model [10–13] and ordinary percolation [15]:

- In isotropic critical systems, conformal transformations, from the half-space to the parabola, of the correlation function and the order parameter profile (with appropriate fixed boundary conditions) show that these quantities become stretched exponential functions of  $x/l_C$  or  $L/l_C$  with a stretching exponent  $1-k$ . According to our mean-field and MC-results, this exponent should be changed into  $1-zk$  in anisotropic critical systems. Conformal methods can no longer be used with anisotropic critical systems for which the conformal group is replaced by the Schrödinger group (when  $z=2$ ) [27].
- In isotropic off-critical systems, the tip order parameter is a stretched exponential function of  $\xi/l_C$  (with there  $l_C = C^{1/(1-k)}$ ) with a stretching exponent  $(1-k)/k$ . This follows from exact results on the Ising model [11,12] and also from an heuristic argument assuming that the tip order, which is induced by the bulk order at a distance  $D \sim (\xi/C)^{1/k}$  (where the width of the system is of the order of the bulk correlation length), decays with  $D$  like the critical tip-to-bulk correlation function [10,11]. The same argument, applied to the anisotropic off-critical system, gives a stretched exponential function of  $\xi_{\parallel}/l_C$  with a stretching exponent  $(1-zk)/zk$ . Such a behaviour could not be checked numerically here, since our finite off-critical system involves some unknown combination of the two scaling variables  $L/l_C$  and  $\xi_{\parallel}/l_c$ .

Further numerical and analytical work on anisotropic systems would be useful to confirm the last point.

## Acknowledgments

We thank S. Blawid and I. Peschel for discussions and collaboration, B. Berche and J. M. Debierre for communicating their Monte-Carlo algorithm. CK thanks Henri Poincaré University for hospitality. This work was supported by CNIMAT under project No 155C93.

## References

- [1] Cardy J L 1983 *J. Phys. A: Math. Gen.* **16** 3617
- [2] Barber M N, Peschel I and Pearce P A 1984 *J. Stat. Phys.* **37** 497
- [3] Cardy J L 1984 *Nucl. Phys. B* **240** 514
- [4] Peschel I 1985 *Phys. Lett.* **110A** 313
- [5] Kaiser C and Peschel I 1989 *J. Stat. Phys.* **54** 567
- [6] Davies B and Peschel I 1991 *J. Phys. A: Math. Gen.* **24** 1293
- [7] Guttmann A J and Torrie G M 1984 *J. Phys. A: Math. Gen.* **17** 3539
- [8] Cardy J L and Redner S 1984 *J. Phys. A: Math. Gen.* **17** L933
- [9] Duplantier B and Saleur H 1986 *Phys. Rev. Lett.* **57** 3179
- [10] Iglói F, Peschel I and Turban L 1993 *Adv. Phys.* **42** 683
- [11] Peschel I, Turban L and Iglói F 1991 *J. Phys. A: Math. Gen.* **24** L1229
- [12] Davies B and Peschel I 1992 *Ann. Phys. (Leipzig)* **2** 79
- [13] Blawid S and Peschel I 1994 *Z. Phys. B* **95** 73
- [14] Turban L and Berche B 1993 *J. Physique I* **3** 925
- [15] Berche B, Debierre J M and Eckle P 1994 *Phys. Rev. E* (to appear)
- [16] Privman V and Švrakić N M 1989 *Directed Models of Polymers, Interfaces and Clusters* Lecture Notes in Physics 338 (Berlin: Springer)
- [17] Binder K and Wang J S 1989 *J. Stat. Phys.* **55** 87
- [18] Turban L 1992 *J. Phys. A: Math. Gen.* **25** L127
- [19] Iglói F 1992 *Phys. Rev. B* **45** 7024
- [20] Kinzel W 1983 *Ann. Israel Phys. Soc.* **5** 425
- [21] Essam J W, Guttmann A J and De'Bell K 1988 *J. Phys. A: Math. Gen.* **21** 3815
- [22] Kaiser C and Turban L 1994 *J. Phys. A: Math. Gen.* **27** L579
- [23] Stauffer D 1985 *Introduction to Percolation Theory* (London: Taylor & Francis) p 64
- [24] Pincus P 1976 *Macromolecules* **9** 386
- [25] de Gennes P G 1979 *Scaling Concepts in Polymer Physics* (Ithaca: Cornell University Press) p 50
- [26] Turban L and Debierre JM 1984 *J. Phys. A: Math. Gen.* **17** L289
- [27] Henkel M 1994 *J. Stat. Phys.* **75** 1023